How anatase TiO_2 with {101} {001} and {100} surfaces affect the photooxidation process of roxithromycin

Zhigang Wei, Shiyun Chen, Yangfei Fang, Zhenrui Wang, Kai Liang, Anselem C. Amakanjaha and Yuanhui Zhong

ABSTRACT

TiO_2 crystals are widely used in photocatalytic processes due to their low cost and fabulous catalytic performance. As described in our previous study, three types of TiO_2 with the main surfaces of {101}, {001} and {100} were synthesized. In this study, the three types of TiO_2 are used to investigate roxithromycin (ROX) photocatalytic degradation kinetics and the pH effect. For photocatalytic degradation, the obtained data have shown that the overall order of optimal degradation is shown as {101} > {001} > {100}. The photooxidation kinetics for {101} facet conforms to first-order kinetics at from pH 5 to pH 10, and most of the photooxidation kinetics for {001} and {100} facets are fitted well with the zero-order and second-order kinetics, respectively. The pH effects are varied to the three types of TiO_2, of which {101} has the best degradation effect at pH values 4, 7 and 8, while {001} works best at pH 5 or pH 6, and {100} has a relatively obvious effect at pH 4 and pH 9. The relation between adsorption and oxidation has been tested and proved that the strong adsorption corresponds to the fast oxidation.

Key words | facet effect, pH effect, photooxidation, roxithromycin, TiO_2

HIGHLIGHTS

- Three types of TiO_2 with the main facets of {101}, {001} and {100} were used to degrade roxithromycin in water solution.
- Based on the results, the catalytic abilities followed the order of {101} > {001} > {100}.
- The photooxidation kinetics were investigated.
- The pH effect was significant to the oxidation.

Zhigang Wei (corresponding author)
Shiyun Chen
Yangfei Fang
Zhenrui Wang
Kai Liang
Anselem C. Amakanjaha
Yuanhui Zhong
School of Chemical Engineering and Light Industry,
Guangdong University of Technology,
Guangzhou, 510006,
China
E-mail: *weizg2003@126.com*

doi: 10.2166/wst.2020.538

GRAPHICAL ABSTRACT

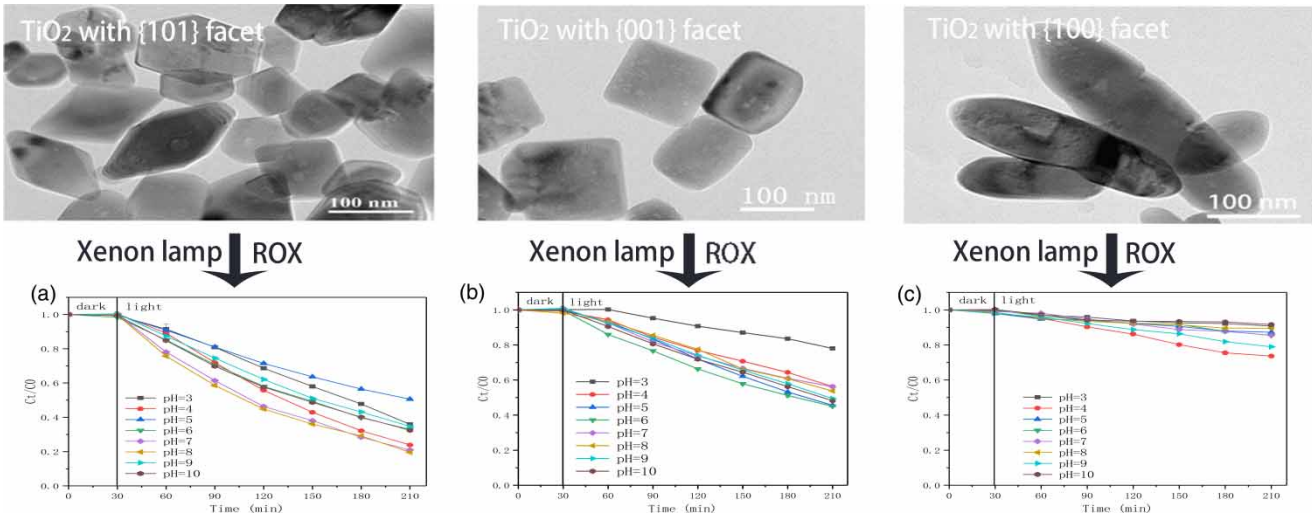

INTRODUCTION

Antibiotics, widely used to treat various diseases due to their abilities of effectively treating bacterial infections and preventing bacterial infections, can be processed into anti-inflammatory drugs, animal feed additives, animal growth promoting agents and sterilizations (Hang *et al.* 2007; Ding *et al.* 2015; Gothwal & Shashidhar 2015). However, more than 30 antibiotics have been found in sewage, surface water and even underground drinking water environment, which were mainly derived from industrial wastewater, medical antibiotics and veterinary antibiotics (Dodd *et al.* 2006; Mahmoud *et al.* 2017). Antibiotics include macrolide antibiotics, tetracycline and its derivative antibiotics, glycoside antibiotics, amino acid and its derivative antibiotics, *β*-lactam antibiotics and so on (Zhang *et al.* 2004). Roxithromycin (ROX), classified as a semi-synthetic 14-membered macrolide antibiotic, has antibacterial activity against Mycoplasma pneumoniae, Chlamydia pneumoniae, and venom (Xu *et al.* 2017). ROX is relatively stable in physical and chemical properties, has strong stability to light, heat and humidity, and has a half-life of 130 days to 180 days in water (Massé *et al.* 2014). It has serious adverse effects on animals, plants and microorganisms in the natural environment, such as the emergence of super bacteria and inhibiting the growth of plant roots and the emergence of drug resistance in humans and animals (Alok *et al.* 2008). Because of their high toxicity and high residues, antibiotics have attracted widespread attention from environmental scholars (Grujić *et al.* 2009). In the report of Gao *et al.*, the concentration of ROX detected at the outlet of the sewage treatment plant was at least 1 μg/L (Gao *et al.* 2012). Peng *et al.* (Peng *et al.* 2011; Yang *et al.* 2011) measured the concentration of ROX in the Guangzhou section of the Pearl River as more than 1 μg/L. Zhou *et al.* (2011) detected the maximum concentration of ROX in the bottom mud of the Haihe River in China, which was as high as 67.2 μg/L. It is shown that currently a large number of ROX has been detected in water bodies and sediments, which are threatening human health. Therefore, research about the degradation of ROX is important and necessary. The chemical structure of ROX is in Figure S1 of the appendix.

TiO_2 crystals are widely used in photocatalytic processes due to their low cost and fabulous catalytic performance (Babić *et al.* 2017). Experiments have shown that controlling the specific exposed surface of TiO_2 can improve the catalytic efficiency of titanium dioxide. Liu *et al.* (2010a) proposed a kind of nanosized anatase TiO_2 single crystal with the {001} facet of 18%, which had a lower band gap and exhibited excellent photocatalytic activity both for generating OH radicals and for splitting water into hydrogen. In 2016, Yan *et al.* (2016) investigated the effect of the distribution of exposed facets in adsorption, and the result showed that anatase {001} facets had stronger adsorption affinity than anatase {101} facets to reduce arsenic. These investigations into facet effect were based on the controlled

synthesis methods of TiO_2. In the recent years, there have been some methods to control the mainly exposing facets of TiO_2 such as {101}, {001} and {100} facets (Han *et al.* 2009; Li & Xu 2010; Pan *et al.* 2011). Amano *et al.* (Amano *et al.* 2009a, 2009b) used P25 and potassium hydroxide to perform a high-temperature and high-pressure hydrothermal reaction in a reactor to prepare potassium titanate nanowires. The synthesized potassium titanate nanowires were used as precursors and successfully synthesized octahedral-shaped anatase titanium dioxide during the hydrothermal reaction, which mostly exposed {101} crystal planes. In 2010, Liu's group (Liu *et al.* 2010b) used titanium powder as a titanium source and hydrofluoric acid solution as a solvent to hydrothermally synthesize the flower-like structure of exposed {001} face titanium dioxide. The experimental results showed that, compared with P25, the flower-like structure {001} facet TiO_2 had a higher photocatalytic degradation performance for methylene blue. In 2012, Li *et al.* (2012) used P25 as a titanium source to hydrothermally synthesize sodium titanate nanotubes in NaOH solvent, and then used sodium titanate nanotubes as precursors to hydrothermally synthesize anatase titania square facet nanometer rods (TFNRs), which mainly exposed the {100} surface, and the result indicated that the {100} surface may play an important role in the photocatalytic reaction. In our recent report (Wei *et al.* 2019), three kinds of anatase TiO_2 crystals with the main facets of {101}, {001} and {100} were synthesized and used to investigate the facet effect and pH effect for reducing arsenic in water.

TiO_2 has been used to degrade ROX in recent years. In 2010, Huo *et al.* (2010) reported the degradation of ROX by poly-o-phenylenediamine/TiO_2/fly ash hollow microbeads. In 2014, Kwiecien *et al.* (2014) proposed the UV-induced TiO_2 photocatalytic degradation of ROX. It is obvious that TiO_2 possesses enough ability to reduce ROX. However, the facet effect and the pH effect, which are the important factors during the reducing process, have not been discussed yet. Therefore, in the present paper, three kinds of anatase TiO_2 crystals with the main facets of {101}, {001} and {100} are used to show the ROX photocatalytic degradation kinetics and the pH effect.

EXPERIMENTAL METHODS

Material and reagents

ROX was obtained from JK Chemical Co., Ltd, China. Degussa titanium dioxide P25 (80% anatase and 20% rutile) was obtained from Chengdu Cloning Chemical Reagent Factory, China. Sulfuric acid (H_2SO_4), hydrochloric acid (HCl), potassium hydroxide (KOH) and sodium hydroxide (NaOH) were purchased from Guangzhou Hualisen Trading Co., Ltd, China. Ammonium nitrate (NH_4NO_3), hexamethylenetetramine ($C_6H_{12}N_4$) and ammonium carbonate ($(NH_4)_2CO_3$) were purchased from Shanghai Chemical Reagent Factory, China. The different TiO_2 crystals have been synthesized as in our previous paper (Han *et al.* 2009; Li & Xu 2010; Pan *et al.* 2011; Wei *et al.* 2019), and the experimental details are in the appendix.

During the experiments, all reagents were analytically pure and the solutions were prepared in distilled water.

Apparatus

Powder X-ray diffraction (XRD, Rigaku-Ultima III) analyses were carried out to determine the crystal structures of the obtained anatase TiO_2. Scanning electron microscope (SEM, JEOL JSM-6700F) and transmission electron microscopy (TEM, JEM-2100F from JEOL. Ltd) analyses were carried out to characterize the morphologies of TiO_2 crystals. The Brunauer-Emmett-Teller (BET, Quantachrome Instruments, USA) analyses gave the specific surface area of three types of TiO_2. The visible spectrophotometer analyses were used to detect the concentrations of ROX, and the detail methods and the standard curves are in the appendix, Figure S2. Liquid chromatography-mass spectrometry (LC/MS, LC/MS-2020 from Daojin, Japan) analyses were used to identify the degradation products of ROX.

Photooxidation process

The photooxidation process of ROX was carried out with a 0.5 L glass flask containing 0.3 g TiO_2 (2,000 mg/L) and 0.25 L of ROX (100 mg/L). 0.1020 g of ROX was dissolved in a volumetric flask of 100 mL with 10 mL 0.01 M HCl, then diluted to the volume with distilled water to obtain 1,000 mg/L solution. 10 mL of 1,000 mg/L ROX was added to a 100 mL volumetric flask, and diluted to the volume with distilled water to obtain the preparation solution. Then the solution with 100 mg/L ROX was adjusted to the desired pH values, such as pH 3 to pH 10, by adding HCl or NaOH. The adsorption equilibrium of ROX was obtained by magnetic stirring for 30 minutes in the dark.

Hydroquinone, ammonium oxalate and isopropanol were added to ROX in order to capture $\blacksquare O^{2-}$, $\blacksquare OH$ and h^+, respectively (Andrei *et al.* 2019). At the same time, the experimental

conditions with $C_{TiO2} = 2{,}000$ mg/L, $C_{ROX} = 100$ mg/L, $C_{hydroquinone} = 0.1$ mmol/L (or $C_{ammonium\ oxalate} = 0.1$ mmol/L or $C_{isopropanol} = 0.1$ mmol/L), and the best pH environments for the oxidation were chosen.

Then, the photooxidation reaction was carried out by two Xenon lamps (285–750 nm, 92.3 mW/cm^2) with an oxygen flux of 1.5 L/min. An aliquot sample of 10 mL was taken from the suspension through a syringe filter of 0.22 μm and sampled at 0, 30, 60, 90, 120, 150, 180, and 210 min (The first 30 minutes were in the dark). All experimental points were tested three times and the average values were taken.

Adsorption process

In order to study the adsorption processes, the concentration of ROX was decreased to 10 mg/L and the concentration of TiO_2 was reduced to 500 mg/L. Then, the best and the worst pH environments for the oxidation were chosen. An aliquot sample of 10 mL was taken from the suspension through a syringe filter of 0.22 μm and sampled at 0, 30, 60, 90, 120, 150, 180, and 210 min. The experiments were conducted in a dark environment.

Kinetics testing

In order to characterize the photooxidation processes of ROX (Li-Ming *et al.* 2004; Zhang *et al.* 2005), the data were based on the relationship with f (C_t) = f (t), f (ln C_t) = f (t) and f ($1/C_t$) = f (t), where C_t was the concentration of ROX at t min and t stood for time, and the order of photooxidation reaction was determined, then the rate constants of k and R^2 about zero-order model, first-order model and second-order model were calculated.

RESULT AND DISCUSSION

Structure and morphology

The different TiO_2 crystals with the main facets of {101}, {001} and {100} have been synthesized with the methods in our previous paper (Han *et al.* 2009; Li & Xu 2010; Pan *et al.* 2011; Wei *et al.* 2019). The experimental details, as well as the XRD, the SEM and the TEM images, were published in our previous work (Wei *et al.* 2019). The BET of the three kinds of TiO_2 were also measured in the order of {101} (21.21 m^2/g) > {001} (19.22 m^2/g) > {100} (17.08 m^2/g). The exposed percent of {101}, {001} and {100} respectively were 91.4, 67.1 and 66.7% (Yu *et al.* 2014). The details are in the appendix (Figure S3).

Photooxidation kinetics

Variations of ROX concentrations before and during Xenon lamp for three types of TiO_2 at pH 7 are shown in Figure 1. It can be seen from Figure 1 that there is no obvious effect for in the dark adsorption of 30 min, which is consistent with Kwiecien's results (Kwiecien *et al.* 2014). And the TiO_2 with {101} facet maintains the best degradation effect in neutral environment, while the TiO_2 with {001} surface is the second and the TiO_2 with {100} facet has the worst effect. A set of low concentration experiments were also carried out, where the concentration of ROX was 5 mg/L and the concentration of TiO_2 was 500 mg/L, such as in Figure S4. It is shown that the photocatalytic oxidation abilities also follow the order of {101} facet > {001} facet > {100} facet, which agree with the results from the high ROX concentration such as 100 mg/L.

The photodegradation efficiencies of ROX are characterized by the zero-order kinetic model, first-order kinetic model and the second-order kinetic model.

The zero-order model is shown below:

$$C_t = C_0 - k_0 t \tag{1}$$

where C_t and C_0 are the photocatalytic concentrations of ROX at reaction time t min and 0 min respectively. k_0 is the zero-order photodegradation rate constant, which is determined by the slope of the linear fit of C_t versus t.

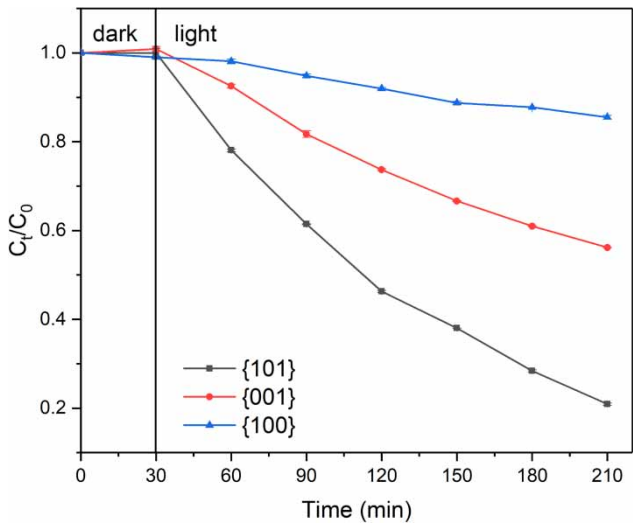

Figure 1 | Variation of ROX concentration before and during Xenon lamp for three types of TiO_2 at pH 7 (The initial ROX is 100 mg/L and TiO_2 is 2.0 g/L).

The model of the first-order rate is as follows:

$$C_t = C_0 \cdot e^{-k_1 t}$$

$$\ln C_t = \ln C_0 - k_1 t \quad (2)$$

where k_1 is the first-order photodegradation rate constant, which is determined by the slope of the linear fit of $\ln C_t$ and t.

The expression of the second-order rate is given as:

$$\frac{1}{C_t} = \frac{1}{C_0} + k_2 t \quad (3)$$

where k_2 is the second-order photodegradation rate constant, which is determined by the slope of the linear fit of $1/C_t$ and t.

The catalytic kinetic data k and the fitness R^2 of the three types of TiO_2 to ROX from pH 3 to pH 10 are presented in Table 1. From Table 1, for {101} facet TiO_2 from pH 5 to pH 10, the photooxidation kinetics conform to the first-order kinetics with the well linear relationship, which is consistent with the results of Kwiecien *et al.* (2014). However, at the low pH values such as pH 3 and pH 4, it is more consistent with the zero-order kinetics.

For {001} facet TiO_2, most of the photooxidation kinetics conform to the zero-order kinetics such as from pH 3 to pH 5 and from pH 8 to pH 10. At pH 6, the first-order kinetics is more suitable for the reaction; at pH 7, the second-order kinetics is the best one.

For {100} facet TiO_2, the results can fit with zero, first and second orders, while the zero-order kinetics are the best for pH values 4, 6, 9 and the second-order kinetics are the best for pH values 3, 5, 7, 8, 10. The speed of reaction rate may be the result of many factors, such as pH value, reactant concentration, temperature, etc. We will focus on the pH effects in the next section.

The pH effects

Figure 2 presents the degradation effects of ROX by Xenon lamp and TiO_2 crystals at pH values from pH 3 to pH 10 after 30 minutes adsorption.

Table 1 | The kinetic constants for ROX on the three types of TiO_2

			Zero-order model		First-order model		Second-order model	
Catalytic	**Concentration of ROX**	**pH**	k_0	R^2	k_1 (×100)	R^2	k_2 (×1,000)	R^2
{101} facet TiO_2 C = 2,000 mg/L	C = 100 mg/L	3	0.3377	0.9976	0.5590	0.9651	0.0990	0.8841
		4	0.4231	0.9868	0.8170	0.9850	0.1805	0.8983
		5	0.2526	0.9918	0.3840	0.9987	0.0603	0.9849
		6	0.3155	0.9821	0.6150	0.9978	0.1296	0.9581
		7	0.3963	0.9543	0.8560	0.9972	0.2165	0.9194
		8	0.3925	0.9408	0.8650	0.9934	0.2255	0.9012
		9	0.3500	0.9888	0.5930	0.9959	0.1081	0.9508
		10	0.3420	0.9779	0.6210	0.9987	0.1222	0.9585
{001} facet TiO_2 C = 2,000 mg/L	C = 100 mg/L	3	0.1258	0.9725	0.1430	0.9663	0.0164	0.9566
		4	0.2076	0.9949	0.3150	0.9904	0.0489	0.9687
		5	0.2883	0.9958	0.4490	0.9869	0.0730	0.9522
		6	0.2841	0.9810	0.4410	0.9993	0.0712	0.9873
		7	0.2109	0.9803	0.3330	0.9962	0.0538	0.9968
		8	0.2062	0.9904	0.3480	0.9822	0.0602	0.9603
		9	0.2466	0.9992	0.3950	0.9910	0.0655	0.9582
		10	0.2651	0.9973	0.4010	0.9944	0.0627	0.9639
{100} facet TiO_2 C = 2,000 mg/L	C = 100 mg/L	3	0.0442	0.9579	0.0493	0.9624	0.0055	0.9666
		4	0.1165	0.9869	0.1720	0.9854	0.0255	0.9809
		5	0.0524	0.9757	0.0638	0.9770	0.0078	0.9776
		6	0.0677	0.9716	0.0818	0.9706	0.0099	0.9680
		7	0.0690	0.9796	0.0859	0.9814	0.0107	0.9825
		8	0.0443	0.9205	0.0517	0.9279	0.0060	0.9346
		9	0.0956	0.9940	0.1230	0.9904	0.0159	0.9845
		10	0.0372	0.7971	0.0438	0.8048	0.0052	0.8124
TiO_2 (Kwiecien *et al.* 2014) C = 1,250 mg/L	C = 100 mg/L	2			0.7680			

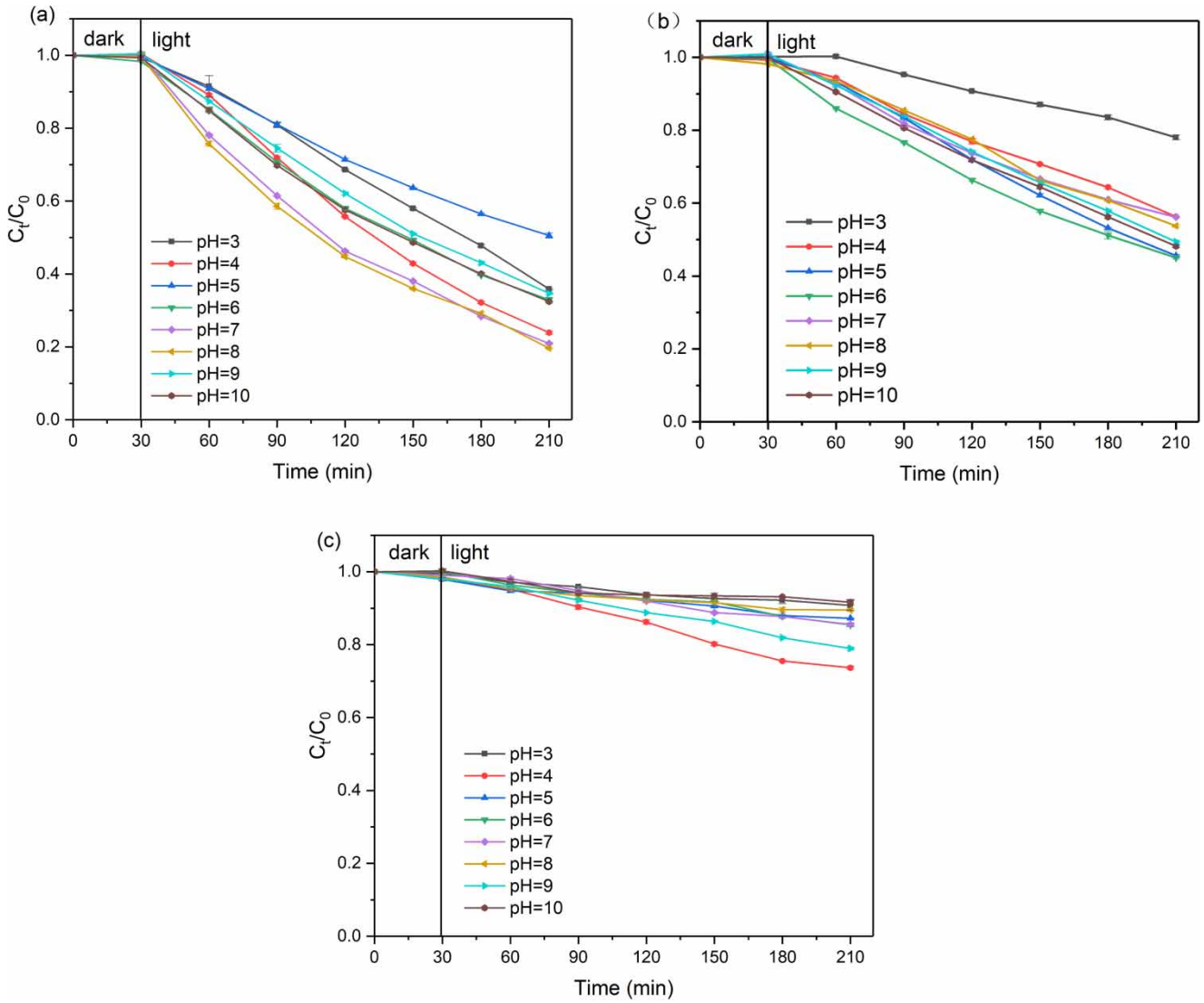

Figure 2 | Photocatalytic oxidation of ROX at different pH values for three types of TiO_2 ((a) is for {101} facet, (b) is for {001} facet, (c) is for {100} facet. The initial ROX is 100 mg/L and TiO_2 is 2.0 g/L).

From Figure 2(a), it can be seen that the best degradation effects by the {101} facet TiO_2 are obtained at pH 4 and pH 7–8, and the lowest point is at pH 8. The kinetics for {101} facet TiO_2 at pH values 4, 7 and 8 are shown in Figure 3, where Figure 3(a) is for zero-order kinetics, Figure 3(b) is for first-order kinetics, and Figure 3(c) is for second-order kinetics. At pH 4, from Figure 3 the zero-order kinetics are more suitable than the first-order and the second-order kinetics with the equation of $C_t = -0.4231t + 94.8285$ and the fitness R^2 of 0.9868. At pH 7 and 8, the first-order kinetics are best with the equations of $\ln C_t = -0.8560 \times 10^{-2}t + 4.5415$ ($R^2 = 0.9972$) and $\ln C_t = -0.8650 \times 10^{-2}t + 4.5220$ ($R^2 = 0.9933$), respectively. It seems that the reaction mechanisms may be different at different pH values.

From Figure 2(b), it is obvious that the best degradation effects by the {001} facet TiO_2 are obtained in weak acidity environments such as at pH 5 and pH 6. The details for {001} facet TiO_2 at pH values 5 and 6 are also shown in Figure 4, where Figure 4(a) is for zero-order kinetics, Figure 4(b) is for first-order kinetics, and Figure 4(c) is for second-order kinetics. At pH 5, from Figure 4 both the zero-order kinetics and the first-order kinetics can fit well with the reaction, and the zero-order kinetics is the best one with the equation of $C_t = -0.2883t + 92.5385$ ($R^2 = 0.9958$). At pH 6, the first-order kinetics is the best fitting for the reaction with the equation of $\ln C_t = -0.0044t + 4.5399$ ($R^2 = 0.9993$).

From Figure 2(c), pH values 4 and 9 possess the best degradation potential for ROX on the TiO_2 with {100} facet.

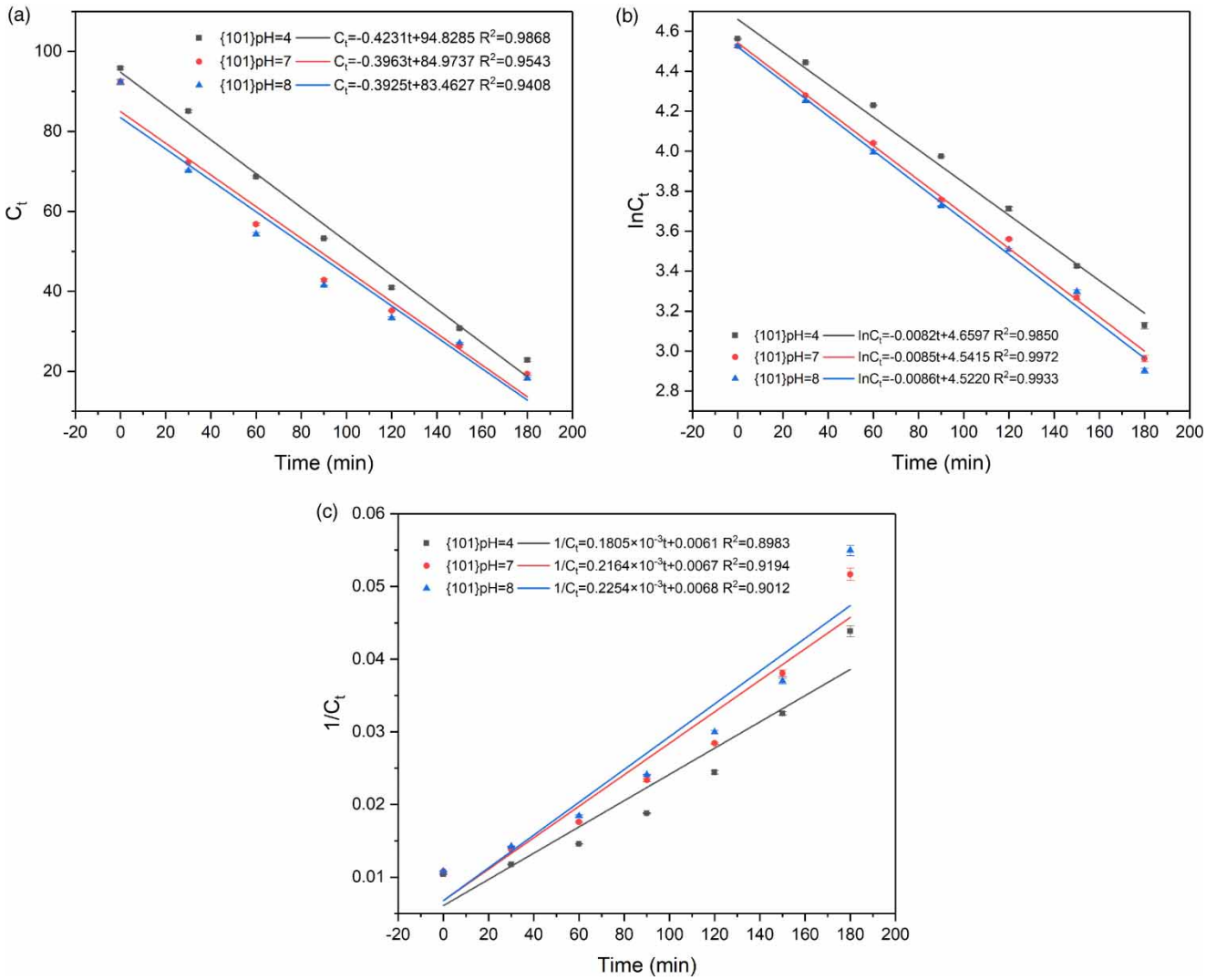

Figure 3 | Zero-order, first-order and second-order kinetics for photocatalytic oxidation on {101} facet TiO_2 at pH 4, pH 7 and pH 8 ((a) is for zero-order kinetics, (b) is for first-order kinetics, (c) is for second-order kinetics. The initial ROX is 100 mg/L and TiO_2 is 2.0 g/L).

However, the {100} facet is so weak for ROX degradation, even at pH 4 the concentration of C_t/C_0 after 180 min is only 0.7364, which is much lower than 0.4501 for {001} facet at pH 6 in Figure 2(b) and 0.1964 at pH 8 for {101} facet in Figure 2(a). The details for {100} facet TiO_2 at pH values 4 and 9 are also shown in Figure 5, where the zero-order kinetics in Figure 5(a) are the best for the reaction with the equations of $C_t = -0.1165t + 78.6433$ ($R^2 = 0.9869$) and $C_t = -0.0956t + 86.7987$ ($R^2 = 0.9940$) for the pH values 4 and 9, respectively.

In summary, the photocatalytic abilities of the TiO_2 facets follow the order of {101} > {001} > {100}, and the best pH value for the {101} facet in our results is 8. Then the MS diagram of the ESI^+ scan of the LC/MS was carried out at pH 8, which is shown in Figure 6. It should be noted that the reaction rate at pH 8 in our experiment, such as in Figure 5(b) $\ln C_t = -0.00865t + 4.5220$ ($R^2 = 0.9933$), is a little faster than that from Kwiecien *et al.*'s result (Kwiecien *et al.* 2014) judging from the reaction rate constant of 0.00768 min^{-1}. Therefore, in Figure 6(b) we chose the same reaction time as Kwiecien *et al.* (2014), such as after 120 min reaction for the LC/MS test. Figure 6(a) shows a scan of ROX and background before the reaction and Figure 6(b) shows the results after 120 min reaction. By comparing Figure 6(a) and 6(b), the new peak m/z 544.50 appears, which stands for the product (c). The structure of product (c) is shown in Figure 6(c), and it had been analyzed by MS/MS technique in some articles (Kwiecien *et al.* 2014;

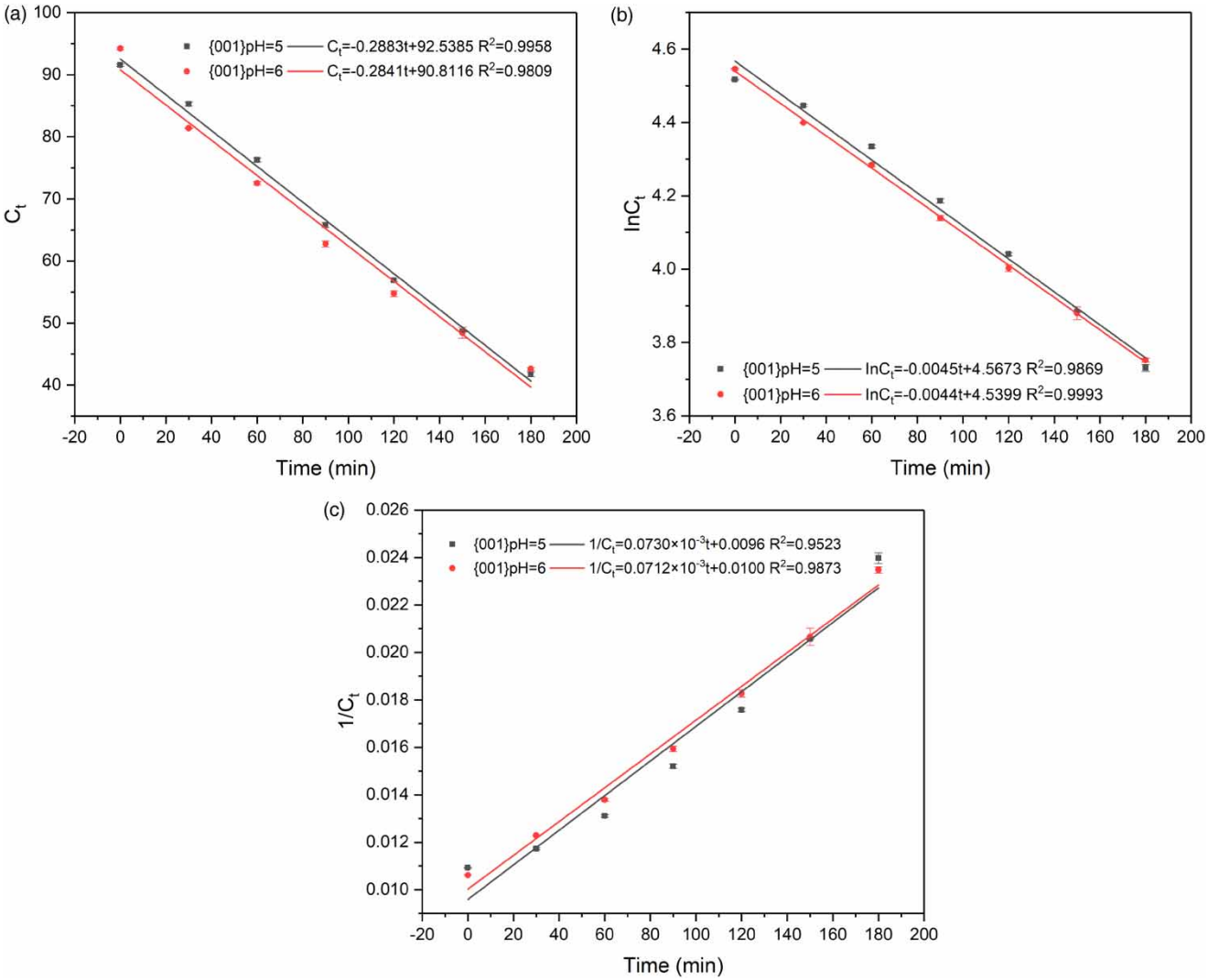

Figure 4 | Zero-order, first-order and second-order kinetics for photocatalytic oxidation on {001} facet TiO_2 at pH 5 and pH 6 ((a) is for zero-order kinetics, (b) is for first-order kinetics, (c) is for second-order kinetics. The initial ROX is 100 mg/L and TiO_2 is 2.0 g/L).

Xu *et al.* 2017). The detailed comparison of Figure 6(a) and 6(b) is in the appendix. It seems that product (c) can be proposed as a product of ROX after 120 min reaction. However, the catalytic process is complicated and the product (c) is only a deduction from the LC/MS results of Figure 6(a) and 6(b). Further research is still needed to know the reaction paths and the whole reaction mechanism.

The results with traps

Hydroquinone, ammonium oxalate and isopropanol were used to capture $\blacksquare O^{2-}$, $\blacksquare OH$ and h^+, respectively (Andrei *et al.* 2019). Then the experimental conditions were $C_{TiO2} = 2{,}000$ mg/L, $C_{ROX} = 100$ mg/L, $C_{hydroquinone} = 0.1$ mmol/L (or $C_{ammonium\ \ oxalate} = 0.1$ mmol/L or $C_{isopropanol} = 0.1$ mmol/L), pH = 8 for {101} facet TiO_2, pH = 6 for {001} facet TiO_2, and pH = 4 for {100} facet TiO_2, and the reaction time was 3 hours, as shown in Figure 2. The results have been collected and shown in Figure 7. In Figure 7, the removal rate is calculated from $(1\text{-}C_t/C_0)$ % and the free capture results are also shown which is the same as that in Figure 2. It is clear that in Figure 7 isopropanol gives the greatest impact on the reaction. Therefore h^+ might be the main oxidant.

The relation between adsorption and oxidation

In our previous research, TiO_2 was used to oxidize arsenite, and the results showed that the catalytic ability of TiO_2 was related to its adsorption ability (Wei *et al.* 2019). Therefore,

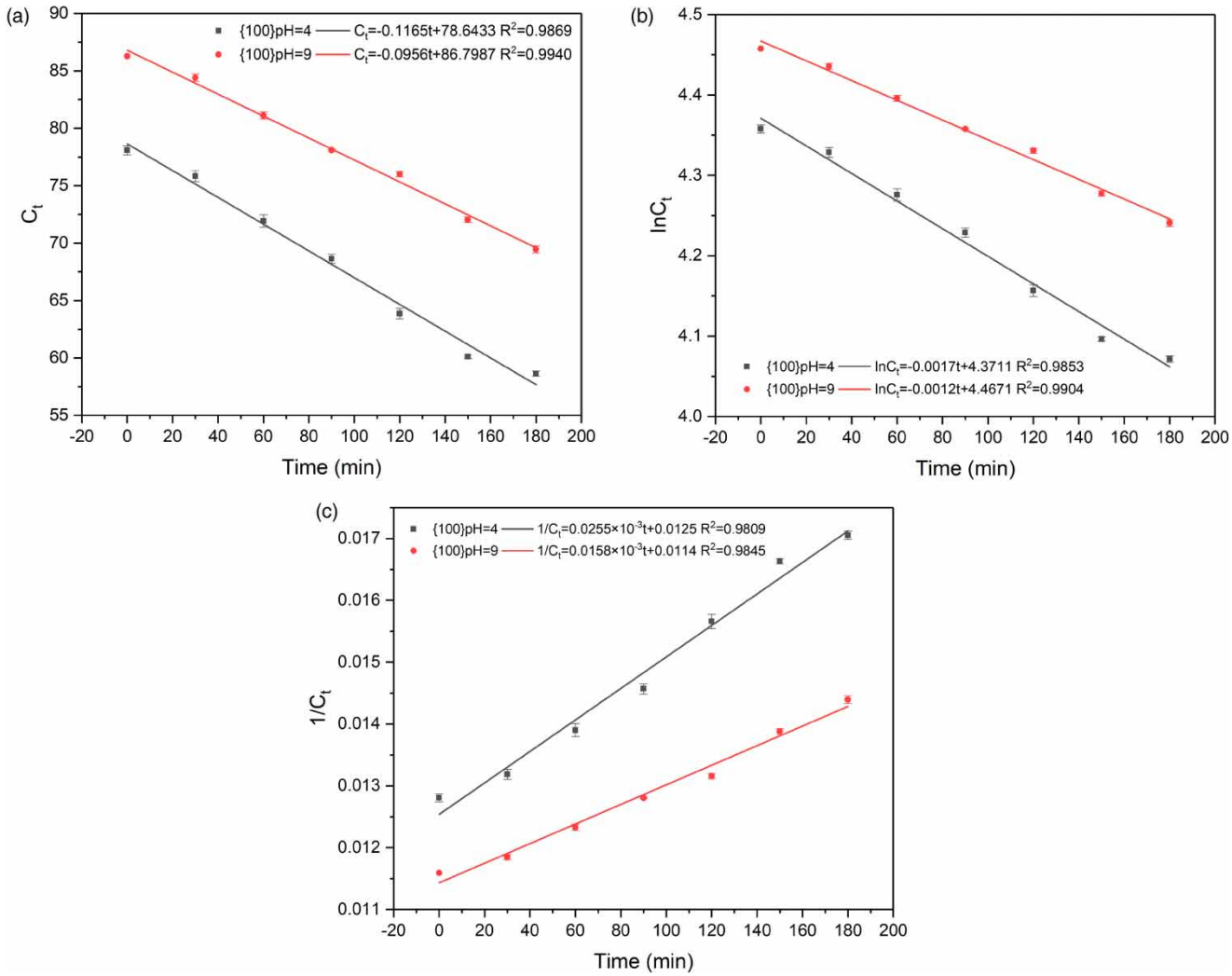

Figure 5 | Zero-order, first-order and second-order kinetics for photocatalytic oxidation on {100} facet TiO_2 at pH 4 and pH 9 ((a) is for zero-order kinetics, (b) is for first-order kinetics, (c) is for second-order kinetics. The initial ROX is 100 mg/L and TiO_2 is 2.0 g/L).

some experiments were carried out to test whether there were some relations between the adsorption and the oxidation for ROX. It has been reported that in the condition such as $C_{ROX} = 100$ mg/L and $C_{TiO_2} = 2{,}000$ mg/L, the adsorption effects were not obvious. In order to study the adsorption processes, the concentration of ROX was decreased to 10 mg/L and the concentration of TiO_2 was reduced to 500 mg/L. Then, the best and the worst pH environments for the oxidation were chosen such as pH 8 and pH 5 for {101} facet TiO_2, pH 6 and pH 3 for {001} facet TiO_2, and pH 4 and pH 3 for {100} facet TiO_2. The results are shown in Figure 8.

By comparing with Figure 2, the better oxidation is corresponding to the stronger adsorption for each kind of TiO_2, such as pH 8> pH 5 for {101} facet TiO_2, pH 6 > pH 3 for {001} facet TiO_2, and pH 4 > pH 3 for {100} facet TiO_2. It should be noted that in Figure 2, the catalytic efficiencies follow the order of pH 8 ({101} facet) ($C_t/C_0 = 0.1964$) > pH 6 ({001} facet) ($C_t/C_0 = 0.4501$) > pH 5 ({101} facet) ($C_t/C_0 = 0.5055$) > pH 4 ({100} facet) ($C_t/C_0 = 0.7364$) > pH 3 ({001} facet) ($C_t/C_0 = 0.7802$) > pH 3 ({100} facet) ($C_t/C_0 = 0.9080$). It is clear that the adsorption ability of TiO_2 generally agrees with its catalytic ability such as pH 8 ({101} facet) (15.22%) > pH 6 ({001} facet) (12.77%) > pH 5 ({101} facet) (11.29%) > pH 4 ({100} facet) (10.20%) > pH 3 ({001} facet) (9.80%) > pH 3 ({100} facet) (4.59%). In addition, the kinetic models such as the pseudo-first order kinetic model, the pseudo-second order kinetic model and the Weber-Morris kinetic model have been used to fit with the data in Figure 8 and the details are listed in the appendix (Figures S5–S7). And the results suggest that the pseudo-second order kinetic is the best one to simulate the adsorption process.

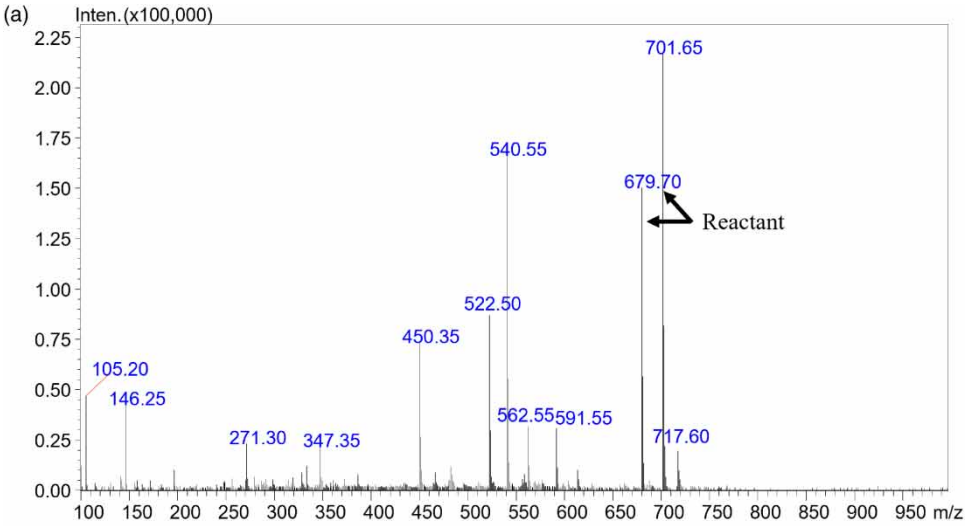

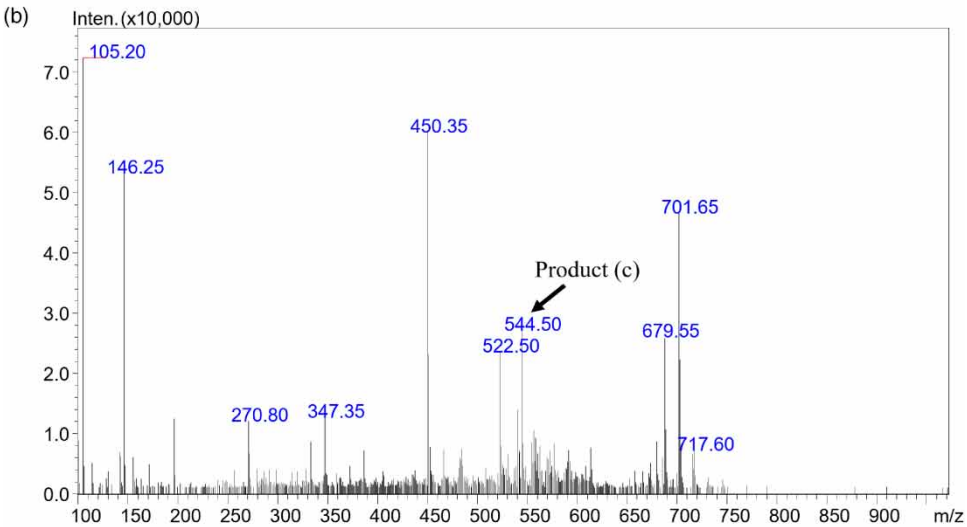

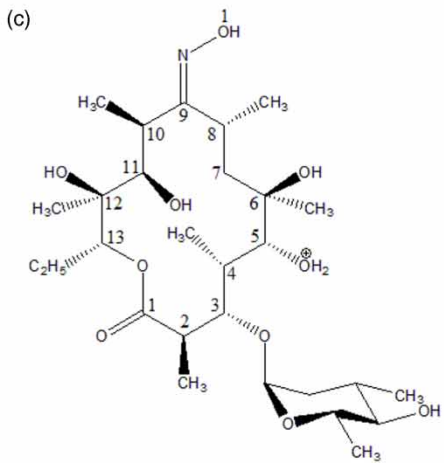

Figure 6 | MS spectra of ROX and photocatalytic degradation product ((a) is for ROX, (b) is for {101} facet after 120 min, (c) is the degradation product of m/z 544.50).

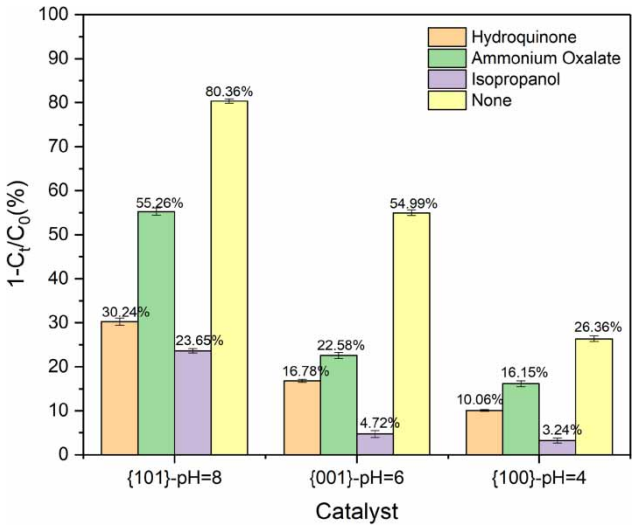

Figure 7 | Removal rate of ROX ((1-C_t/C_0) %) with and without three types of traps. (C_{TiO_2} = 2,000 mg/L, C_{ROX} = 100 mg/L, $C_{hydroquinone}$ = 0.1 mmol/L (or $C_{ammonium\ oxalate}$ = 0.1 mmol/L or $C_{isopropanol}$ = 0.1 mmol/L), pH = 8 for {101} facet TiO_2, pH = 6 for {001} facet TiO_2, and pH = 4 for {100} facet TiO_2, and the reaction time is 3 hours as in Figure 2).

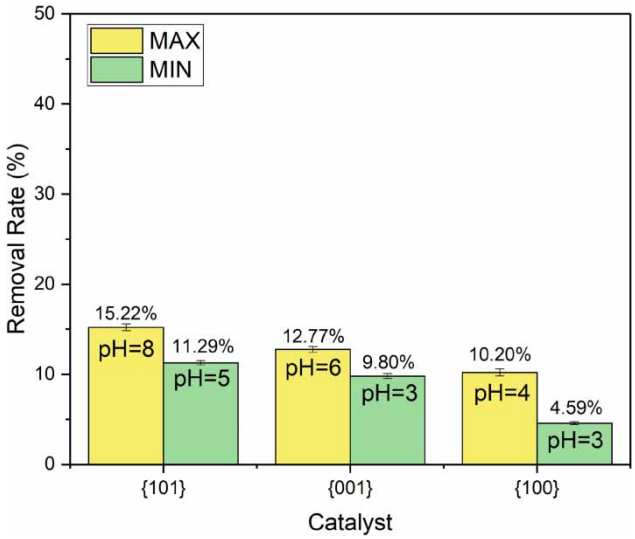

Figure 8 | The adsorption experiments for ROX (Time = 240 min, C_{ROX} = 10 mg/L and C_{TiO_2} = 500 mg/L).

CONCLUSION

In this paper, the photooxidation of ROX on three types of TiO_2 has been studied. It shows that the catalytic abilities of the three types of TiO_2 follow the order of {101} > {001} > {100}. From pH 5 to pH 10, the photooxidation of ROX on the {101} facet follows the first-order kinetics, whereas the {001} and {100} facets obey the zero-order and second-order kinetics, respectively, at most of the pH values. The {101} facet possesses the highest photooxidation rate for ROX at pH 8; the {001} facet works best at pH 5 and pH 6; and the {100} facet has a relatively obvious effect at pH 4. Based on these results, the photooxidation reaction of ROX possesses both a facet effect and pH effect, then the {101} facet at the pH value of 8 is the most favorite condition. A product has also been suggested based on the LC/MS results. However, further work about the reaction mechanism is still needed. Furthermore, the results with traps and adsorption show that h^+ might be the main oxidant, and the catalytic ability of TiO_2 is related with its adsorption ability. Comparing with pseudo-first order kinetic model and Weber-Morris kinetic model, the pseudo-second order kinetic is the best one to simulate the ROX adsorption process on TiO_2.

ACKNOWLEDGEMENTS

The financial supports of this work are the National Natural Science Foundation of China (21373104, 21173022, 20803014), the National Natural Science Foundation of Guangdong Province (2016A030313704), and the Guangdong University funding program (201911845135, 201911845184).

DATA AVAILABILITY STATEMENT

All relevant data are included in the paper or its Supplementary Information.

REFERENCES

Alok, B., Larry, I. C., Wongee, K., Robert, P. H., David, E. K. & Rao, Y. S. 2008 Occurrence of ciprofloxacin, sulfamethoxazole, and azithromycin in municipal wastewater treatment plants. *Practice Periodical of Hazardous, Toxic, and Radioactive Waste Management* **12** (4), 275–281.

Amano, F., Yasumoto, T., Prieto-Mahaney, O. O., Uchida, S., Shibayama, T. & Ohtani, B. 2009a Photocatalytic activity of octahedral single-crystalline mesoparticles of anatase titanium(IV) oxide. *Chemical Communications* **45** (17), 2311–2313.

Amano, F., Yasumoto, T., Shibayama, T., Uchida, S. & Ohtani, B. 2009b Nanowire-structured titanate with anatase titania characterization and photocatalytic activity. *Applied Catalysis B: Environmental* **89** (3–4), 583–589.

Andrei, I., Marina, R., Varsha, S., Vladimir, P., Tetiana, D., Svitlana, N., Vladimir, P., Ahmad, H.-B., Hai, N. T. & Mika, S. 2019 Effect of metal ions adsorption on the efficiency of

methylene blue degradation onto $MgFe_2O_4$ as Fenton-like catalysts. *Colloids and Surfaces A* **571**, 17–26.

Babić, S., Ćurković, L., Ljubas, D. & Čizmić, M. 2017 Tio_2 assisted photocatalytic degradation of macrolide antibiotics. *Current Opinion in Green and Sustainable Chemistry* **6**, 34–41.

Ding, J., Lu, G., Liu, J. & Zhang, Z. 2015 Evaluation of the potential for trophic transfer of roxithromycin along an experimental food chain. *Environmental Science and Pollution Research* **22** (14), 10592–10600.

Dodd, M. C., Buffle, M. O. & Von Gunten, U. 2006 Oxidation of antibacterial molecules by aqueous ozone: moiety-specific reaction kinetics and application to ozone-based wastewater treatment. *Environmental Science & Technology* **40** (6), 1969–1977.

Gao, L., Shi, Y., Li, W., Niu, H., Liu, J. & Cai, Y. 2012 Occurrence of antibiotics in eight sewage treatment plants in Beijing, China. *Chemosphere* **86** (6), 665–671.

Gothwal, R. & Shashidhar, T. 2015 Antibiotic pollution in the environment: a review. *CLEAN – Soil, Air, Water* **43** (4), 479–489.

Grujić, S., Vasiljević, T. & Laušević, M. 2009 Determination of multiple pharmaceutical classes in surface and ground waters by liquid chromatography–ion trap–tandem mass spectrometry. *Journal of Chromatography A* **1216** (25), 4989–5000.

Han, X. G., Kuang, Q., Jin, M. S., Xie, Z. X. & Zheng, L. S. 2009 Synthesis of titania nanosheets with a high percentage of exposed (001) facets and related photocatalytic properties. *Journal of the American Chemical Society* **131** (9), 3152–+.

Hang, T. J., Zhang, M., Song, M., Shen, J. P. & Zhang, Y. D. 2007 Simultaneous determination and pharmacokinetic study of roxithromycin and ambroxol hydrochloride in human plasma by LC-MS/MS. *Clinica Chimica Acta* **382** (1–2), 20–24.

Huo, P., Yan, Y., Songtian, L. I., Huarning, L. I. & Huang, W. 2010 Preparation of poly-o-phenylenediamine/TiO_2/fly-ash cenospheres and its photo-degradation property on antibiotics. *Applied Surface Science* **256** (11), 3380–3385.

Kwiecien, A., Krzek, J., Zmudzki, P., Matoga, U., Dlugosz, M., Szczubialka, K. & Nowakowska, M. 2014 Roxithromycin degradation by acidic hydrolysis and photocatalysis. *Analytical Methods* **6** (16), 6414–6423.

Li, J. M. & Xu, D. S. 2010 Tetragonal faceted-nanorods of anatase TiO_2 single crystals with a large percentage of active {100} facets. *Chemical Communications* **46** (13), 2301–2303.

Li, J., Cao, K., Li, Q. & Xu, D. 2012 Tetragonal faceted-nanorods of anatase TiO_2 with a large percentage of active {100} facets and their hierarchical structure. *CrystEngComm* **14** (1), 83–85.

Li-Ming, H. E., Zhang, H. W. & Zeng, X. H. 2004 Determination of roxithromycin in roxithromycin capsules by UV spectrophotometry. *Academic Journal of Guangdong College of Pharmacy* **20** (5), 475–477.

Liu, G., Sun, C., Yang, H. G., Smith, S. C., Wang, L., Lu, G. Q. & Cheng, H. M. 2010a Nanosized anatase TiO_2 single crystals for enhanced photocatalytic activity. *Chemical Communications* **46** (5), 755–757.

Liu, M., Piao, L., Lu, W., Ju, S., Zhao, L., Zhou, C., Li, H. & Wang, W. 2010b Flower-like TiO_2 nanostructures with exposed {001} facets: facile synthesis and enhanced photocatalysis. *Nanoscale* **2** (7), 1115–1117.

Mahmoud, W. M. M., Rastogi, T. & Kümmerer, K. 2017 Application of titanium dioxide nanoparticles as a photocatalyst for the removal of micropollutants such as pharmaceuticals from water. *Current Opinion in Green and Sustainable Chemistry* **6**, 1–10.

Massé, D., Saady, N. & Gilbert, Y. 2014 Potential of biological processes to eliminate antibiotics in livestock manure: an overview. *Animals* **4** (2), 146–163.

Pan, J., Liu, G., Lu, G. M. & Cheng, H. M. 2011 On the true photoreactivity order of {001}, {010}, and {101} facets of anatase TiO_2 crystals. *Angewandte Chemie-International Edition* **50** (9), 2133–2137.

Peng, X., Zhang, K., Tang, C., Huang, Q., Yu, Y. & Cui, J. 2011 Distribution pattern, behavior, and fate of antibacterials in urban aquatic environments in South China. *Journal of Environmental Monitoring* **13** (2), 446–454.

Wei, Z., Fang, Y., Wang, Z., Liu, Y., Wu, Y., Liang, K., Yan, J., Pan, Z. & Hu, G. 2019 Ph effects of the arsenite photocatalytic oxidation reaction on different anatase TiO_2 facets. *Chemosphere* **225**, 434–442.

Xu, Z., Xu, S., Li, N., Wu, F., Chen, S., Lu, W. & Chen, W. 2017 Waste-to-energy conversion on graphitic carbon nitride: utilizing the transformation of macrolide antibiotics to enhance photoinduced hydrogen production. *ACS Sustainable Chemistry & Engineering* **5** (11), 9667–9672.

Yan, L., Du, J. & Jing, C. 2016 How TiO_2 facets determine arsenic adsorption and photooxidation: spectroscopic and DFT studies. *Catalysis Science & Technology* **6** (7), 2419–2426.

Yang, J.-F., Ying, G.-G., Zhao, J.-L., Tao, R., Su, H.-C. & Liu, Y.-S. 2011 Spatial and seasonal distribution of selected antibiotics in surface waters of the Pearl Rivers, China. *Journal of Environmental Science and Health, Part B* **46** (3), 272–280.

Yu, J., Low, J., Xiao, W., Zhou, P. & Jaroniec, M. 2014 Enhanced photocatalytic CO_2-reduction activity of anatase TiO_2 by coexposed {001} and {101} Facets. *Journal of the American Chemical Society* **136** (25), 8839–8842.

Zhang, S. Q., Xing, J. & Zhong, D. F. 2004 pH-dependent geometric isomerization of roxithromycin in simulated gastrointestinal fluids and in rats. *Journal of Pharmaceutical Sciences* **93** (5), 1300–1309.

Zhang, Y., Ling, L. & Chen, Y. 2005 Study on the dissolubility of roxithromycin capsules and tablets from different manufacturers. *Fujian Medical Journal* **27** (3), 132–134.

Zhou, L.-J., Ying, G.-G., Zhao, J.-L., Yang, J.-F., Wang, L., Yang, B. & Liu, S. 2011 Trends in the occurrence of human and veterinary antibiotics in the sediments of the Yellow River, Hai River and Liao River in northern China. *Environmental Pollution* **159** (7), 1877–1885.

First received 1 August 2020; accepted in revised form 27 October 2020. Available online 9 November 2020